Optimization of Powertrain Platform for Electric Passenger Vehicles

1st Meng Lu
Divison of Industrial Electrical Engineering and Automation
Lund University
Lund, Sweden
meng.lu@iea.lth.se

2nd Gabriel Domingues-Olavarría
Divison of Industrial Electrical Engineering and Automation
Lund University
Lund, Sweden
gabriel.domingues@iea.lth.se

3rd Hannes Bydén
Divison of Industrial Electrical Engineering and Automation
Lund University
Lund, Sweden
hannes.byden@iea.lth.se

4th Mateski Aleksandar
BorgWarner Inc.
Auburn Hills, USA
amateski@borgwarner.com

5th Mats Alakula
Divison of Industrial Electrical Engineering and Automation Lund University
Lund, Sweden
mats.alakula@iea.lth.se

2023 IEEE Transportation Electrification Conference & Expo (ITEC) | 979-8-3503-9742-0/23/$31.00 ©2023 IEEE | DOI: 10.1109/ITEC55900.2023.10187120

***Abstract*— This paper presents a method to optimize an electric powertrain platform, capable of addressing the needs of a wide range of vehicle types while taking advantage of economies of scale and reducing time to market. The optimization includes all electric powertrain components from the electrical machine and inverter to the transmission. The objective is to minimize both the operational and electrical machine cost. Detailed scalable powertrain models are developed and the Particle Swarm Optimization algorithm (PSO) is applied to achieve the optimal design. Results show the benefits and limitations of adopting a platform approach depending on the volumes of the specific applications.**

Keywords—powertrain platform, optimization, PMSM

I. INTRODUCTION

Powertrain optimization for electric vehicles has emerged as a significant area of research in recent years. Most of the academic literature has focused on the modelling and optimizing the different components of the powertrain separately. For example, a methodology to quickly estimate the performance of an electrical machine (EM) by changing the length, outer radius and number of turns of a base design is presented in [1] and a set of scaling rules for permanent magnet machines is described in [2] and used in [3] [4] to find an optimal electrical machine for the applications under study. Similarly, a methodology to estimate the dimensions, performance, and manufacturing cost of the main components in a power electronics converter is shown in [5] and that work takes advantage of pre-existing knowledge on the sizing of semiconductor devices [6], inductors and transformers [7], and modelling of manufacturing processes [8].

The transmission also plays a crucial role in determining the efficiency and performance of the electric powertrain. In [9],the transmission model calculates its losses for each speed and torque, and is calibrated with experiments. in [10], detailed equations to estimate the transmission losses are listed.

Electric powertrains and their components are the subject of numerous research studies aimed at optimizing their performance. However, there is a limited amount of literature that explores the platform-based design for electric powertrains, which is a critical topic for the automotive industry as it can significantly reduce the development time and cost of powertrains by sharing common components across multiple vehicle applications. In [11], powertrain optimization methods are applied to demonstrate how cross-platform optimization can help the original equipment manufacturers (OEMs) create product strategies that are cost effective across a variety of vehicle classes. In [12], a design method able to consider multiple electric powertrain design problems and reduce the system costs by utilizing commonalities between the single designs is proposed.

The benefits of platform-based powertrain optimization are not limited to the automotive industry alone. This strategy can also have positive effects on the environment and society as a whole. By reducing the development time and cost of powertrains, automakers can bring electric vehicles to market more quickly and at more affordable prices, making them more accessible to a larger segment of the population.

This paper provides detailed models of electrical traction machines, power electronic converters, and mechanical transmission, which enable a detailed analysis of powertrain optimization. The proposed powertrain optimization methodology allows us to find the most suitable powertrain design for specific electromobility applications by utilizing the detailed models. Furthermore, the study investigates the advantages and limitations of the platform-based powertrain optimization by exploring the feasibility of having a powertrain platform for three different vehicle classes.

979-8-3503-9742-0/23/$31.00 ©2023 IEEE

II. Methodology

To perform the platform-based powertrain optimization, an electrical machine database containing a large number (100's to 1000's) of EMs with different 2D geometries is prerequisite, where each machine is simulated under the same assumptions.

Fig. 1 illustrates the platform-based powertrain optimization process. One EM 2D geometry is selected from the database as the input of optimization process. It can be scaled to generate new machines using three scaling factors [13]: k_a, which is the ratio between the active length of the scaled EM and the length of base motor in database; N_t, the desired number of turns; and k_{ov}, the ratio between the peak and nominal current. The optimizer will find the optimal machine length, number of winding turns and current rating for the EM, together with the designed inverter and transmission, to minimize the objective function f_1. The vehicle requirement are compared with the designed powertrain performance, and the one which cannot cover all the requirements is discarded. This result provides the optimal design for each vehicle. Once all EMs in the database are evaluated for all vehicle types, the 2D motor geometry that provides the lowest objective function f_2 is selected as the best solution for the platform. Note that for each vehicle type the optimal platform design has the same 2D motor geometry but different length, number of turns and overloading factor.

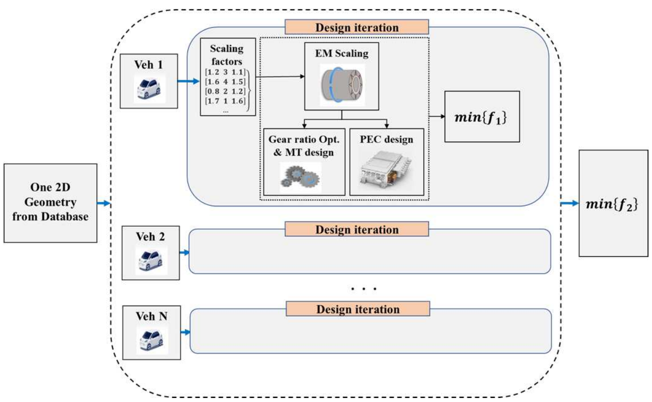

Fig. 1. Powertrain optimization methodology

The optimization problem for the inner most loop can be formulated as expressed in (1), which is defined as Scenario 1, to find the optimal design for each vehicle.

$$\begin{aligned} &min \quad f_1(EM_{ind}, x) \\ &x = (k_a, N_t, k_{ov}) \\ &s.t{:}\, k_a > 0, \quad k_a \in R \\ &\quad N_t > 0, \quad N_t \in N \\ &\quad k_{ov} > 1, \quad k_{ov} \in R \\ &\quad G_m(x) < 0 \end{aligned} \tag{1}$$

Where EM_{ind} is the index of the EM 2D geometry from the database and x is the scaling factor vector. G_m represents all powertrain specific constraints such as performance and overloading requirements, gear ratio limitations, maximum allowed temperatures, etc.

The outer most loop of the optimization can be formulated as shown in (2), which is defined as Scenario 2, to find the optimal platform powertrain design.

$$min \;\; f_2(EM_{ind}) = \sum_{i=1}^{N}[V_i \cdot min\{f_1(EM_{ind}, x)\}] \tag{2}$$

Where V_i represents the intended yearly volumes of each vehicle type, and the number of vehicle types to optimize for is depicted by N. All constraints are evaluated for the different vehicles in the inner most loop. For scenario 2, the production volumes for many of the manufacturing steps are increased, in relation to the different vehicle volumes, to account for the benefits of economies of scale. Thus requiring a unique optimization run.

III. Powertrain Component Modelling

A. Electrical Machine

In this work a V-shape Interior Permanent Magnet Synchronous Motor (VIPMSM) with hairpin windings is used as Fig. 2 presents a parametrized geometry of the EM.

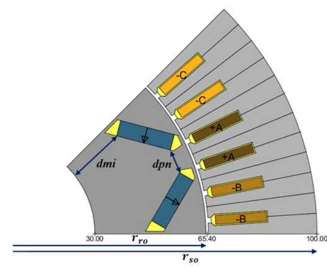

Fig. 2. Example of PMSM with parameterized geometry

TABLE I. EM DATABASE

Parameter	Values	Unit
r_{so}	[80; 90; 100; 110; 120]	mm
r_{ro}/r_{so}	[0.6; 0.65]	-
N_p	[6; 8]	-
q	[2; 3]	-
Relative slot size	[0.9; 0.95; 1]	-
dmi	[0.4; 0.45; 0.5] $(r_{ro} - r_{ri})$	mm
dpn	[0.08; 0.1; 0.12] $(2\pi r_{ro}/N_p)$	mm

Using the parameterized values listed in Table I, a database of 1080 different 2D EM geometries is generated with FEMM, which is an open-source finite element analysis tool [14]. Various parameters are modified to create the EM database, including the stator outer radius (r_{so}), the ratio between rotor and stator outer radius (r_{ro}/r_{so}), the number of poles (N_p), the number of slots per pole and phase (q), the ratio defining the slot size (relative slot size), the distance between v-magnet-slot edge and rotor inner radius (dmi), the distance between the v-magnet-slot edges of the neighbor pole magnets (dpn). The default active length of EMs in the database is set to 150 mm, and number of serial turns is set to 1. All EMs in this paper is assumed to have a liquid cooled water jacket.

After collecting data on torque, current, flux linkage, and flux density from FEMM, the EM losses and efficiency map can be derived through post-processing. This is accomplished using the maximum torque per ampere (MTPA) control algorithm, as described in [13]. Fig. 3 displays the MTPA points represented by dots.

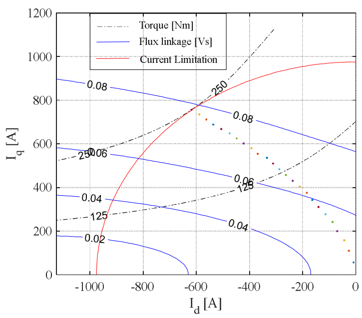

Fig. 3. Torque and flux linkage contour lines in the $[i_d, i_q]$ plane

As discussed in the optimization methodology, the EM scaling is a method used to efficiently create new machines based on existing ones in the database while ensuring accuracy. During the scaling process, the thermal constraints should be satisfied. Then a lumped parameter thermal model based on the previous work in [13] is introduced, as shown in Fig. 4, to take the thermal performance into account.

By utilizing this thermal model with the predefined thermal settings such as coolant temperature, heat transfer coefficient of the cooling system, and maximum allowed winding temperature, the nominal current of each scaled EM at nominal operating point, and the peak current can be estimated.

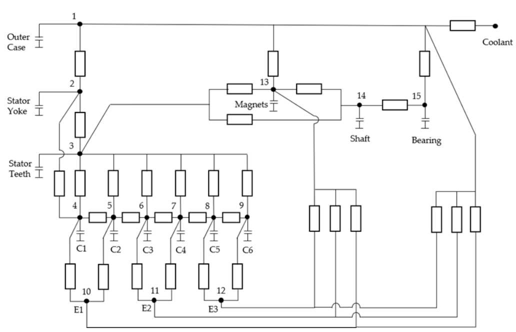

Fig. 4. Lumped parameter thermal model for PMSM

The EM cost is influenced by two primary factors: the cost of materials and the cost of the major manufacturing operations involved in generating and assembling the physical components of the machine. The materials used in constructing the machine are a significant determinant of its cost. However, the cost of manufacturing operations also plays an important factor. These operations, such as blanking, winding, and assembly, etc. require skilled labor and specialized equipment, which is highly dependent with production volumes. Fig. 5 presents the cost distribution for an EM with a production volume of 10 k, as derived from the EM cost model developed in [8]. The figure illustrate both the material cost distribution and the cost distribution with manufacturing.

Fig. 6 illustrates the relationship between the EM cost and the annual production volume. The marginal effect of the decrease in EM price gradually weakens as production volume increases.

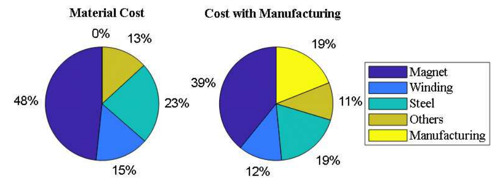

Fig. 5. Cost distribution for a PMSM with production volume of $10k$

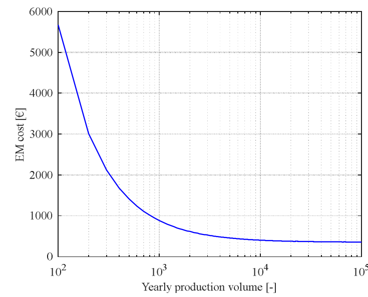

Fig. 6. EM cost vs yearly production volume

B. Inverter

The loss calculation for the inverter is based on scalable electro-thermal models of power modules [15]. For each machine, an iterative process calculates the minimum semiconductor chip size required by first calculating the losses at the most challenging operating point. The thermal resistance of the device is estimated based on the power module materials and the chip size together with assumptions of heat spreading and chip-chip interaction. The junction temperature is then calculated from the losses and thermal resistance. SiC-MOSFET is used in this paper and the power modules are assumed to be liquid cooled with a heat transfer coefficient of 8 kW/m^2K, and the temperature of the coolant is set to 65 °C.

The scalable resistance, on-state voltage and switching loss models were created by extracting data from manufacturer datasheets of several power modules from same generation and with the same packaging. Linear coefficients were used to compensate the turn-on, turn-of and on-state resistance dependence on junction temperature. The inverter design process is shown in Fig. 7.

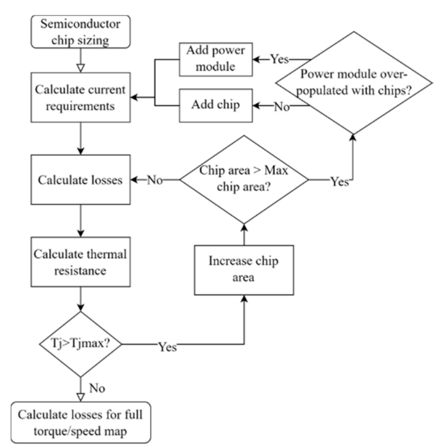

Fig. 7. Flowchart of inverter design

The switching and conduction losses for the power modules can be estimated by (3) and (4).

$$P_{sw} = f_{sw} E_{ref}(I, A_{chip}) \left(\frac{V_{cc}}{V_{ref}}\right)^{K_v} \left(1 + T_{c,sw}(T_j - T_{ref})\right) \tag{3}$$

$$P_{cond} = \left(\frac{1}{8} + \frac{m \cdot \cos(\phi)}{3\pi}\right) R_{on}(A_{chip}) \cdot \hat{I}^2 \left(1 + T_{c,ron}(T_j - T_{ref})\right) \tag{4}$$

In equation (3), the switching losses are estimated. The switching frequency is denoted as f_{sw}. The operating temperature and blocking voltage are represented by T_j and V_{cc}, respectively. T_{ref} and V_{ref} are the reference values at which the energy losses are defined in the datasheet. T_c and K_v are the temperature and voltage compensation constants. The energy losses during a switch event are represented by E_{ref}.

The conduction losses are computed by (4). m is the modulation index, $\cos(\phi)$ is the power factor of the EM, R_{on} is the electrical resistance for the power modules, $\hat{I}$ is the phase peak current of the EM.

C. *Transmission*

In this paper, a transmission model has been adapted based on the work in [16] that accurately determines the appropriate size for each of the components, including gears, shafts, and bearings. The model also calculates the corresponding loss and efficiency maps. The model is capable of sizing both single and multi-speed transmissions with parallel or transverse architectures.

This paper also focuses on the method of improving the energy consumption via optimizing the final gear ratio [17], then the electric vehicle can work at more efficient operating points.

For a single-speed transmission, given that the traction motor is able to deliver the required power, the gear ratio should be constrained as shown in (5), by the torque and speed requirements.

$$\frac{T_{max,wheel}}{T_{max,EM}} \leq g_r \leq \frac{n_{max,EM}}{n_{max,wheel}} \tag{5}$$

From all the available gear ratios, the one that results in the lowest energy consumption is chosen as the input for the detailed transmission model.

IV. Case Study

A. *Electric Vehicle Specificaitons*

A total of 3 vehicle classes have been defined to investigate platform-based powertrain optimization. Each vehicle has its own specifications, which are from the industry partner, and are shown in Table II. They are all propelled by a single electric traction machine with a single-speed transmission to evaluate the vehicle energy consumption and electrical machine cost in different degrees of electrical machine commonality.

TABLE II. VEHICLE SPECIFICATIONS

Parameter	**Class A**	**Class B**	**Class C**
Weight (kg)	1280	1480	1850
Front area (m^2)	2.11	2.20	2.36
Drag Coefficient	0.32	0.31	0.267
Rolling resistance	0.008	0.008	0.008
Max speed (km/h)	180	180	180
Acceleration 0-100kph (s)	< 10	< 9	< 8
Overtaking 80-120kph (s)	< 6	< 4	< 3
Gradeability	7% @180 kph 25% @40 kph		

According to the vehicle performance requirements in Table II, the required torque on wheel side is calculated, as shown in Fig. 8. These figures offer a clear understanding of the torque required to achieve the vehicle performance and the designed powertrain performance should cover all the operating points. The WLTP drive cycle is applied to evaluate the optimization results.

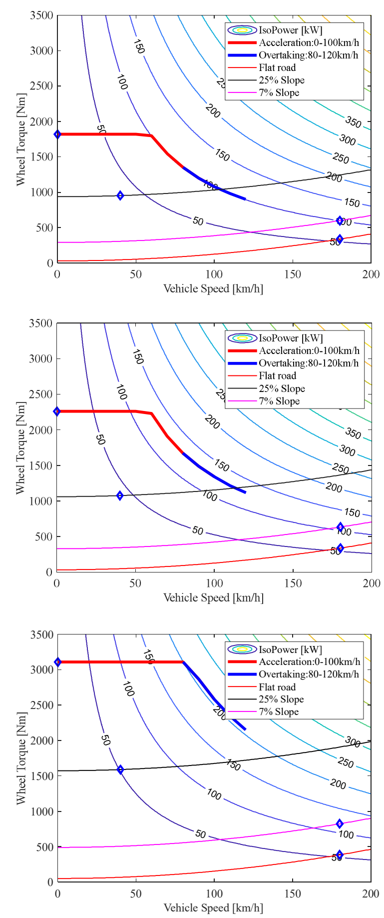

Fig. 8. Vehicle requirement on wheel side for Class A, B and C

B. *Objective Function and Constraints*

For the presented case study, the relationship between EM and operational cost is to be explored. For this reason, the objective function for the inner most loop $f_1(x)$ is defined as shown in (6), where the EM cost is denoted as C_{EM} and the operating cost as C_{Op}. The weighting factor k_c determines the relative importance of the two objectives in $f_1(x)$. Besides the performance requirements previously established, a minimum overloading time of 30s and a maximum gear ratio of 16 are set as optimization constraints as it can be seen in (6).

$$f_1(EM_{ind}, x) = C_{EM}(EM_{ind}, x) \cdot k_c + C_{Op}(EM_{ind}, x) \cdot (1 - k_c) \qquad (6)$$

$$t_{ov} > 30s$$

$$g_{r,max} < 16$$

The operating cost C_{Op} for each vehicle is estimated based on energy consumption over one year with an assumed annual mileage of 20,000 km and the electricity price of 0.3€/kWh.

V. Results

In this section, the proposed methodology and models are applied in the optimization for the three vehicle classes.

The objective function allows for exploring different weightings between the two objectives. As an example of results for a single application, Fig. 9 illustrates the optimization results for the Class C vehicle, where two weighting factors were applied to the objective function. Each circle on the graph represents the optimal powertrain configuration for a specific 2D EM geometry. The results clearly demonstrate that when the EM cost is prioritized ($k_c = 1$), the optimizer tends to minimize the EM cost at the expense of operating cost. When k_c is set to 0, a higher initial EM cost and lower operating costs is achieved.

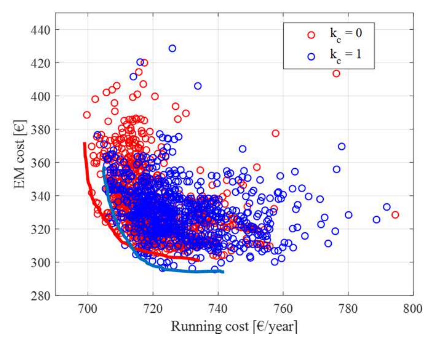

Fig. 9. Powertrain designs with different weigting factors for Class C

The powertrain platform study is performed by optimizing the powertrain for each vehicle with the two scenarios. The yearly production volume for scenario 1 is set to 10 k units/year per vehicle class. Figure 10 shows the results for the inner most optimization loop when f_1 is evaluated at both 10 k and 30 k units/year. The first set of results represent the optimal solution for scenario 1, with the optimal solution marked with star in the pareto front for each vehicle class. While the second set of results are used to compute f_2 in order to calculate the optimal solution for scenario 2 as shown in Fig. 11.

Since scenario 2 employs a shared 2D EM topology for all vehicles, it results in lower EM cost due to the larger economies of scale. However, the system efficiency is compromised, leading to higher operating costs compared with the results from scenario 1. Furthermore, as it should be expected, the optimal solution for scenario 2 does not lay in the pareto front for f_1 evaluated at $30k$ units/year, as shown in Fig. 10, as it is a compromised solution. The EM geometries for all applications are shown in Table III.

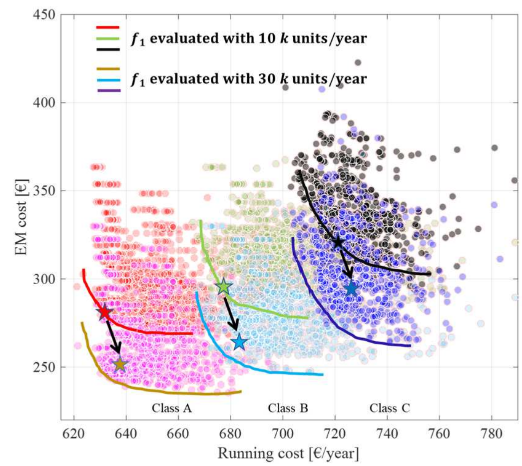

Fig. 10. Optimization results for all vehicles in scenario 1 with different production volumes.

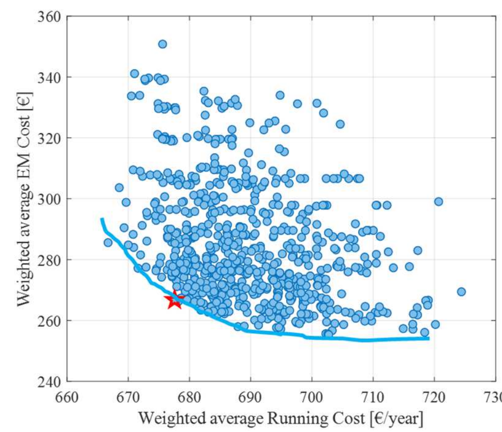

Fig. 11. Optimization results for all vehicles in scenario 2.

TABLE III. EM GEOMETRIES WITH TWO SCENARIOS

Scenario 1			Scenario 2
Class A	***Class B***	***Class C***	***Class A&B&C***
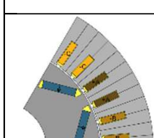 $\varnothing 200 \times 129mm$	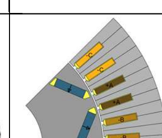 $\varnothing 220 \times 110mm$	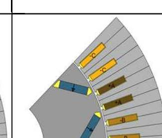 $\varnothing 240 \times 120mm$	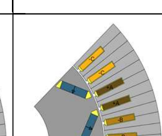 $\varnothing 220 \times (96\&110\&166)mm$

Table IV shows the relation between the EM production volume and the cost of one EM from Class C.

TABLE IV. EM COST VS EM YEARLY PRODUCTION VOLUME

	EM yearly production volume (Units)				
	1k	***10k***	***30k***	***100k***	***300k***
EM cost (€)	806	327	294	283	280

With a limited EM production volume, the EM cost can be up to 2~3 times higher than that with higher volume. The EM cost decreases from 327€ to 294€ as production volumes increase from $10k$ to $30k$, which can also be seen in Fig. 10. With further production volume increases, there comes a point where the cost reduction of the EM is not significant despite the increase improved economies of scale. That being said, this does not includes the benefits of reduced development cost, which have a significant impact even at mid to high volumes. This aspect will be investigated in detail in a future publication.

To illustrate the design details, the optimal powertrain design for Class C with scenario 1 is shown in Table V.

TABLE V. POWERTRAIN DESIGN FOR CLASS C WITH SCENARIO 1

EM 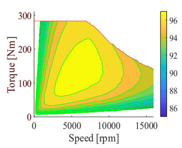	Active length	$120mm$
	Num. of turns	4
	Num. of winding layers	8
	Num. of parallel paths	4
	Nominal torque/power	$240Nm/186kW$
	Max torque/power	$282Nm/209kW$
Transmission 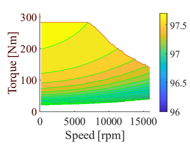	Gear ratio	10.97
	Num. of teeth for gear stage 1	32/113
	Num. of teeth for gear stage 2	37/115
Inverter 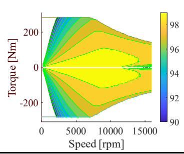	Power modules	SiC
	Num. of chips	5
	Single chip area	$54\ mm^2$

VI. CONCLUSIONS AND FUTURE WORK

The results show that the detailed models and optimization methodology presented can be used to design more efficient and cost-effective powertrains for specific applications with enough details. The study on powertrain platform across different vehicle classes also provide valuable insights into the potential benefits of platform-based powertrain design in the electromobility industry. Platform-based design allows for the sharing of common components across multiple vehicle applications, resulting in reduced cost, especially for low volume applications. Additionally, adopting platform approaches allows to reduce development cost, validation effort and time to market. However, the study also highlights the challenges and limitations associated with the adoption of a platform strategy, such as compromises in powertrain efficiency, as each vehicle class has its own unique requirements. When dealing with applications with high production volume, the marginal benefits derived from economies of scale tend to decline. A methodology like the one presented in this paper allows to accurately depict at which volumes the benefits of developing powertrain platforms outweight the drawbacks and viceversa, which is essential for informed decision making around powertrain strategy.

To make this study more comprehensive, the detailed transmission and inverter cost models are required in the future. It is also necessary to explore deeper into objectives that are challenging to quantify, such as the powertrain development time and the R&D cost.

REFERENCES

[1] Z. Kan, A. Ivanco, Z. Filipi and H. Hofmann, "Finite-Element-Based Computationally Efficient Scalable Electric Machine Model Suitable for Electrified Powertrain Simulation and Optimization," IEEE Transactions on Industry Applications, vol. 51, no. 6, p. 4435–4445, 2015.

[2] S. Stipetic, Z. Damir and P. Mircea, "Scaling laws for synchronous permanent magnet machines," in Tenth International Conference on Ecological Vehicles and Renewable Energies (EVER), 2015.

[3] D. Žarko, M. Kovačić, S. Stipetić and D. Vuljaj, "Optimization of electric drives for traction applications," in 19th International Conference on Electrical Drivesand Power Electronics (EDPE), 2017.

[4] R. Kesavan, S. Stipetic, M. Gobbi and G. Mastinu, "Optimal sizing of traction motors using scalable electric machine model," IEEE Transactions on Transportation Electrification, vol. 4, pp. 314-321, 2018.

[5] G. Domingues-Olavarría, P. Fyhr, A. Reinap, M. Andersson and M. Alaküla, "From Chip to Converter: A Complete Cost Model for Power Electronics Converters," IEEE Transactions on Power Electronics, vol. 32, no. 11, pp. 8681-8692, 2017.

[6] R. Burkart and J. Kolar, "Component cost models for multi-objective optimizations of switched-mode power converters," in 2013 IEEE Energy Conversion Congress and Exposition, 2013.

[7] N. Mohan, T. Undeland and R. William, Power electronics: converters, applications, and design, John wiley & sons, 2003.

[8] P. Fyhr, Electromobility: Materials and Manufacturing Economics, Lund University, 2018.

[9] P. Caillard, G. Frederic, H. Michel, R. Sid-Ali and N. Janiaud, "An Optimization Methodology to Pre-Design an Electric Vehicle Powertrain," in 2014 IEEE Vehicle Power and Propulsion Conference (VPPC), 2014.

[10] Koch, A, Nicoletti, L, Herrmann, T and Lienkamp, M. "Implementation and Analyses of an Eco-Driving Algorithm for Different Battery Electric Powertrain Topologies Based on a Split Loss Integration Approach," Energies 2022, 15, 5396.

[11] B. Falvy and M. Bryant, "Cross-platform electric powertrain optimisation for developing modular product families," Drive System Design.

[12] D. Lechleitner, M. Hofstetter and M. Hirz, "Cost Reduction of Electric Powertrains by Platform-Based Design Optimization," 2020 IEEE Transportation Electrification Conference & Expo (ITEC), Chicago, IL, USA, 2020, pp. 139-146.

[13] M. Lu, G. Domingues-Olavarría, F. J. Márquez-Fernández, P. Fyhr and M. Alaküla, "Electric Drivetrain Optimization for a Commercial Fleet with Different Degrees of Electrical Machine Commonality," Energies 2021, 14, 2989.

[14] "FEMM-homepage" Available: https://www.femm.info/wiki/HomePage. [Accessed 15 April 2023].

[15] H.Bydén, E. Bourniche, A. Leblay and M. Alakula, "Electro-thermal Models of Power Modules for Stochastic Optimization of Inverters," unpublished.

[16] J. H. Olsson, J. Lundborg, Transmission modeling for Optimization of Electric Powertrains, Lund University, 2021.

[17] Koch, A.; Teichert, O.; Kalt, S.; Ongel, A.; Lienkamp, M. "Powertrain Optimization for Electric Buses under Optimal Energy Efficient Driving," Energies 2020, 13, 6.